SELF-HEATING OF 1d THERMAL PLASMA;

COMPARISON OF WEIGHTINGS; OPTIMAL PARAMETER CHOICES

by

A. Peiravi and C. K. Birdsall

Memorandum No. UCB/ERL M78/32

12 June 1978

ELECTRONICS RESEARCH LABORATORY

College of Engineering
University of California, Berkeley
94720

ABSTRACT

Self-heating times of a one dimensional electrostatic simulation thermal plasma are presented using zero order weightings (NGP), linear weighting (CIC-PIC), and quadratic spline weighting (QS). Maximum heating times are found to be along $v \frac{\Delta t}{\Delta x} \approx \frac{3}{2}$ for NGP and $\approx \frac{1}{2}$ for CIC and QS. Considerable increase in self-heating time is achieved through truncation in k-space.

Research sponsored by the Department of Energy Contract EY-76-S-03-0034-PA128.

I. INTRODUCTION

The self-heating (nonphysical) times for one-dimensional electrostatic thermal plasma are presented using zero order weighting (NGP), linear weighting (CIC-PIC), and quadratic spline weighting (QS) in a momentum conserving* code, ES1 of A. B. Langdon [1]. The self-heating time τ_h is defined as the time taken for the thermal energy of the system to double. A 1d electrostatic thermal plasma model consisting of a mobile electron species and immobile neutralizing ion background was used. For this system, this is the time in which the average kinetic energy of an electron increases by $\frac{1}{2}\kappa T$. The increase in energy is numerical in origin and stochastic in nature. It arises from fluctuations in the force due to the presence of finite grids in space and time. Thus, the self-heating times strongly depend on Δt and Δx.

A Maxwellian velocity loader with first and second moment correction was used [2].

R. W. Hockney [3] empirically obtained the self-heating times for a 2d plasma with ions and electrons using $T_e = T_i$, $m_i/m_e = 64$, with further refinement by Hockney et al., [4]. We have added quadratic spline weighting and show self-heating times are longest for $v_t\frac{\Delta t}{\Delta x} \simeq \frac{3}{2}$ for NGP and $v_t\frac{\Delta t}{\Delta x} \simeq \frac{1}{2}$ for CIC and QS.

*Energy conserving codes also show self-heating for $\Delta t \neq 0$. Only in the limit of $\Delta t \rightarrow 0$ is energy conserved.

II. CHOICE OF $\omega_p \Delta t$: DETERMINATION OF SELF-HEATING TIME τ_h

Typical growths in time of the thermal energy are shown for NGP in Fig. 1 (cases A1-A6).* For $\omega_p \Delta t \leq 0.6$ the energy increases linearly with time, implying a random process; the remaining work presented will be for $\omega_p \Delta t$ in this range. For larger $\omega_p \Delta t$, the growth in thermal energy is like t^n, but with $n > 1$, which implies some other kind of growth, as yet unexplained. The same change in growth pattern for $\omega_p \Delta t \geq 0.6$ was observed for CIC-PIC and QS weightings. From histories like those of Fig. 1, with slope of one, $\omega_p \tau_h$ was determined.

Figure 1 shows raw data and does not have points at early time. When we plot all the points from $t = 0$ onward on a linear plot, then we see fluctuations preceding linear growth in time; these are due to the ordered (but not quiet) start. In obtaining τ_h, the zero in time and initial thermal energy were assigned to the beginning of growth linear in time.

---

*See Appendix C for the parameters for each case.

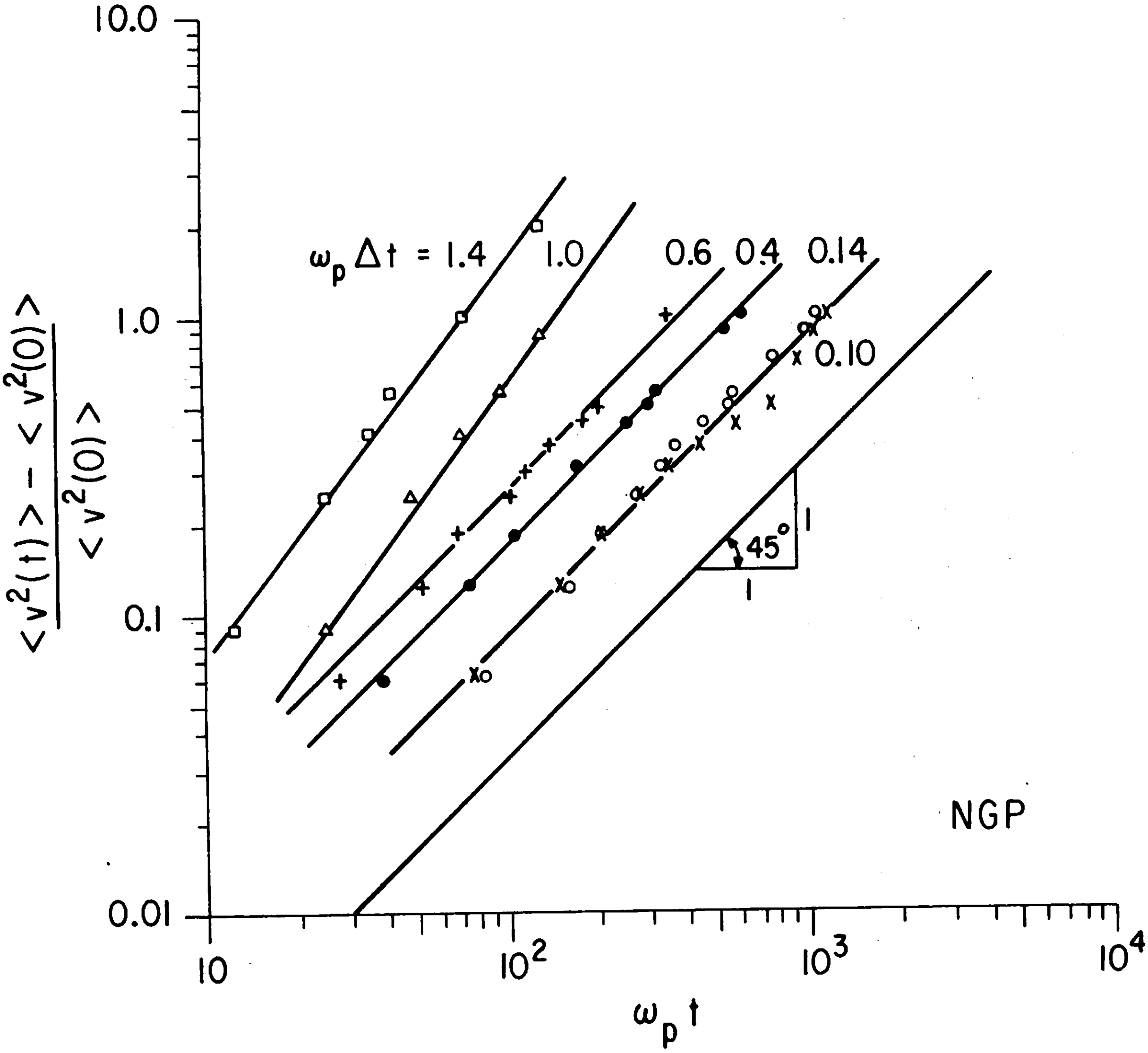

Fig. 1. Increase in $\langle v^2(t)\rangle/\langle v^2(0)\rangle$ with time for zero-order weighting (NGP) scheme, for several values of $\omega_p \Delta t$ with $\lambda_D/\Delta x = 1.0$. The $\langle\ \rangle$ means average over all particles. The heating time τ_h is defined as the time for $\langle v^2(t)\rangle$ to double, that is, when the curve reaches 1.0.

III DEPENDENCE ON $n_o\lambda_D$, $n_o\Delta x$, $n_o(\lambda_o + \Delta x)$

The self-heating times are plotted in Fig. 2 in units of electron plasma frequency, $\omega_p\tau_h$, vs $N_D = n_o\lambda_D$ and $N_C + N_D = n_o(\Delta x + \lambda_D)$ (cases A7-A11, B1-B5) where n_o is varying. Fig. 3 shows $\omega_p\tau_h$ vs $N_C + N_D$ for two different ratios of $\lambda_D/\Delta x$ where n_o is no longer varying but λ_D and Δx are varied using NGP (cases A27-A28 for $\lambda_D/\Delta x = 2$ and A12-A15 for $\lambda_D/\Delta x = 0.5$) Similar behavior is observed for CIC. These figures lead to the conclusion that for a fixed $\lambda_D/\Delta x$, $\omega_p\tau_h$ is proportional to $N_C + N_D$.

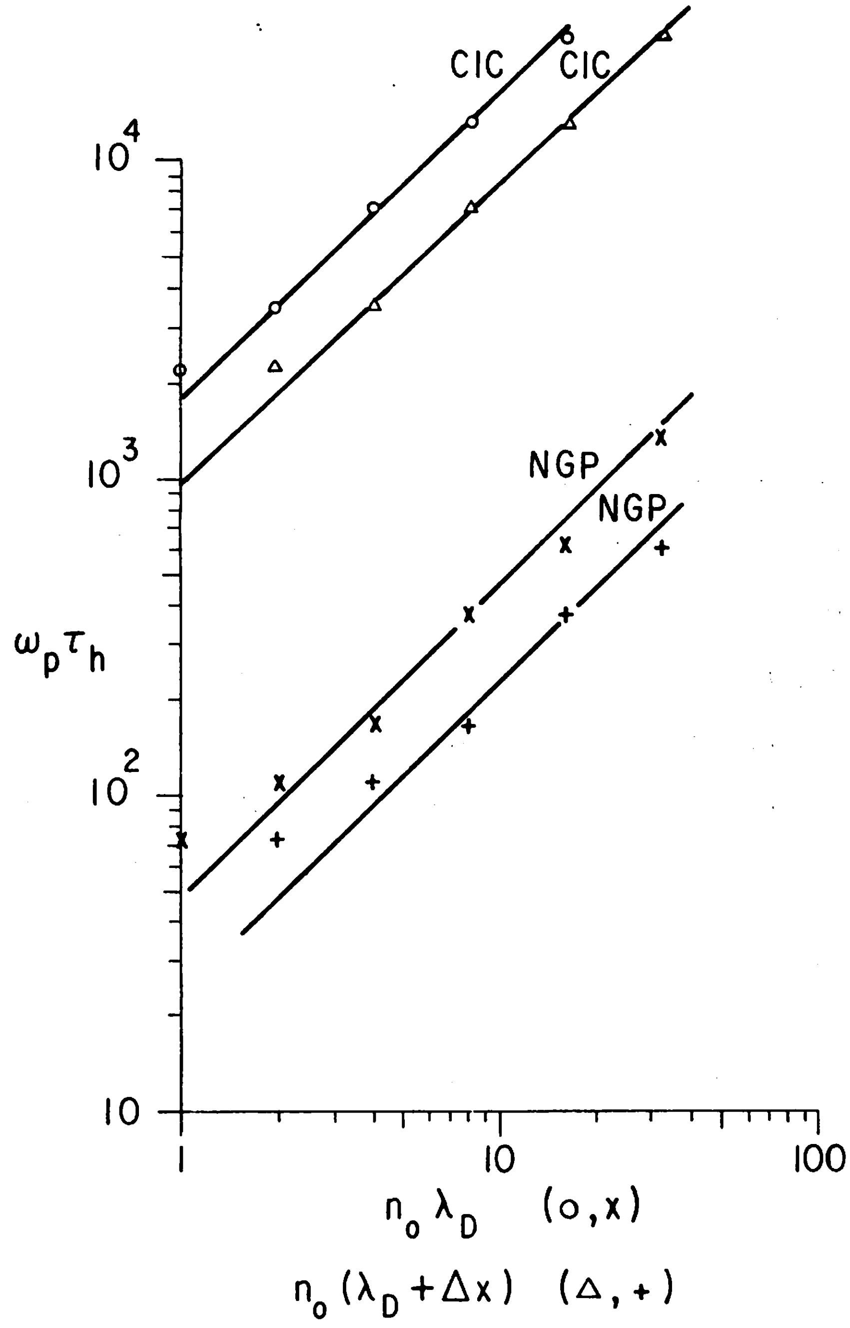

Fig. 2. Self-heating time vs $n_o\lambda_D$ or $n_o(\lambda_D + \Delta x)$ for NGP, CIC showing linear dependence.

Fig. 3. Self-heating time vs $N_C + N_D$ for different $\lambda_D/\Delta x$ ratios showing linear dependence of $\omega_p\tau_h$ on $N_C + N_D$ for fixed $\lambda_D/\Delta x$ for NGP.

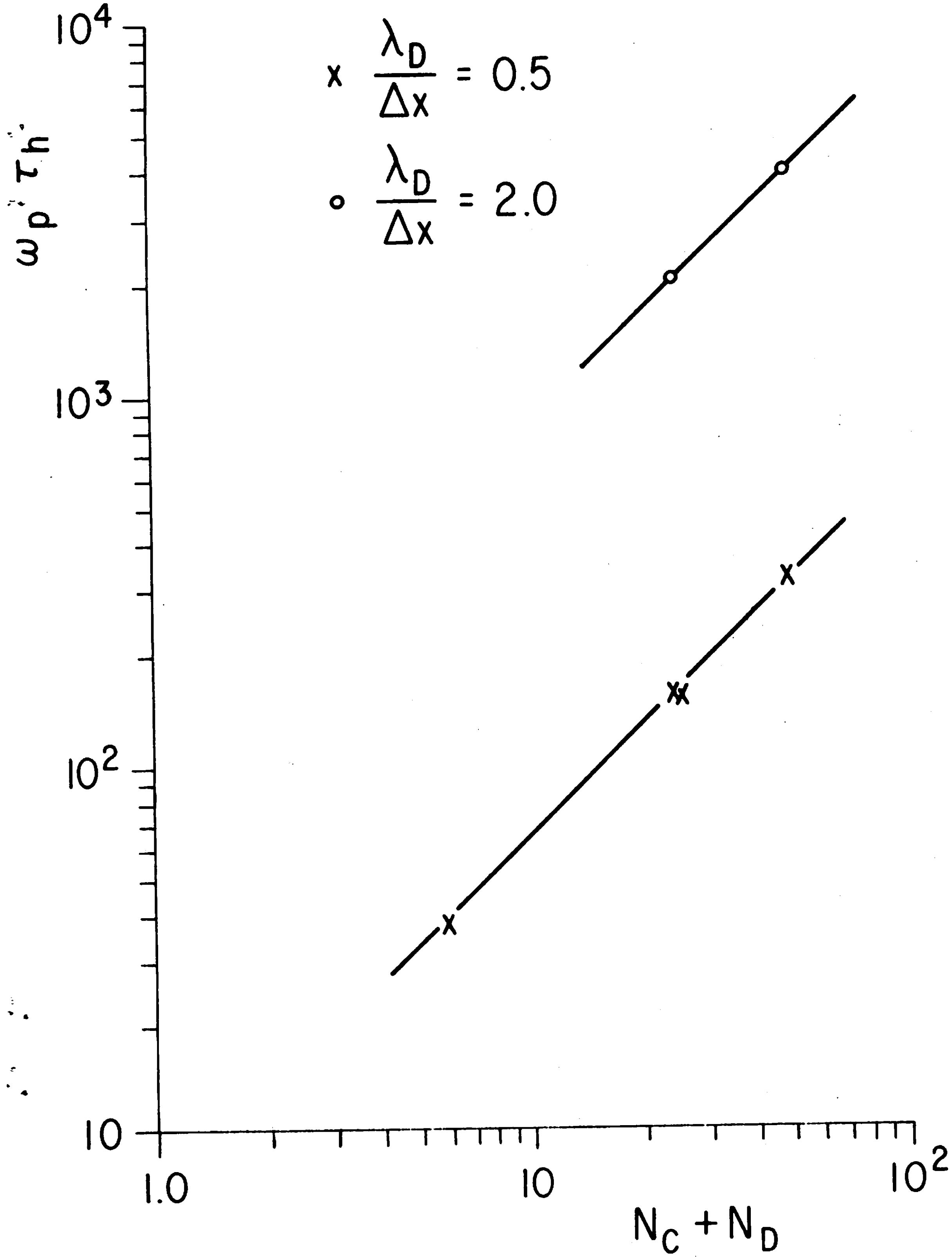

IV DEPENDENCE ON $\lambda_D/\Delta x$; OPTIMUM CHOICE OF $v_t \frac{\Delta t}{\Delta x}$

The self-heating times $\omega_p \tau_h$ divided by $N_C + N_D$ are plotted in Figs. 4, 5 and 6 vs $\lambda_D/\Delta x$ for different values of $\omega_p \Delta t$ (cases A16-A63, B6-B60, C1-C42). The dashed line drawn through the different graphs is $v_t \frac{\Delta t}{\Delta x} \simeq \frac{3}{2}$ for NGP and $v_t \frac{\Delta t}{\Delta x} \approx \frac{1}{2}$ for CIC and QS. The longest heating times occur near these values of $v_t \frac{\Delta t}{\Delta x}$.

Fig. 4. Self-heating times divided by $N_C + N_D$ vs $\lambda_D/\Delta x$ for several $\omega_p\Delta t$ for NGP.

Symbol	+	○	×	□	△
$\omega_p\Delta t$	0.1	0.2	0.4	0.5	0.6

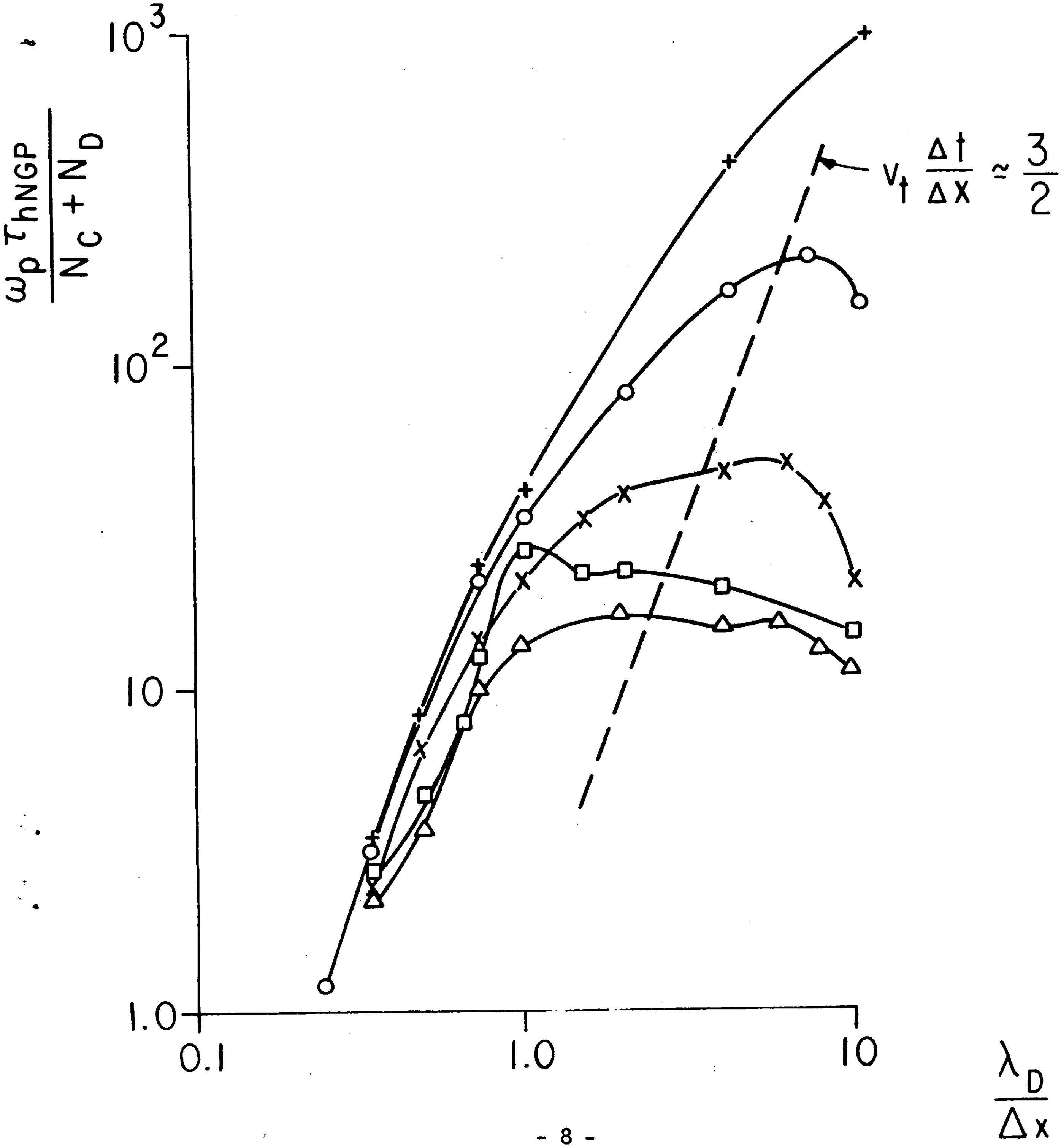

Fig. 5. Self-heating times divided by $N_C + N_D$ vs $\lambda_D/\Delta x$ for several $\omega_p \Delta t$ for CIC

Symbol	+	○	—	×	□
$\omega_p \Delta t$	0.1	0.2	0.3	0.4	0.5

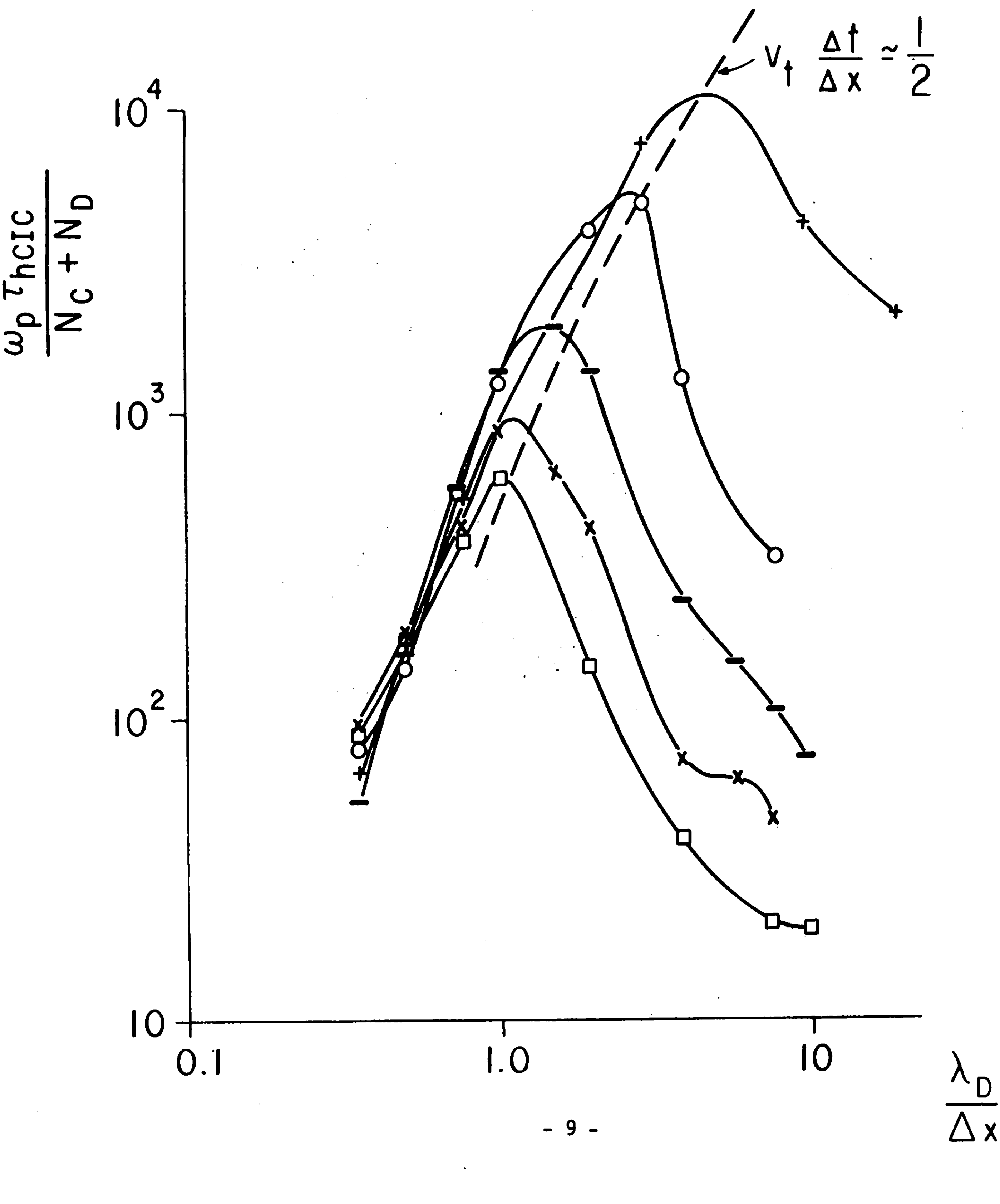

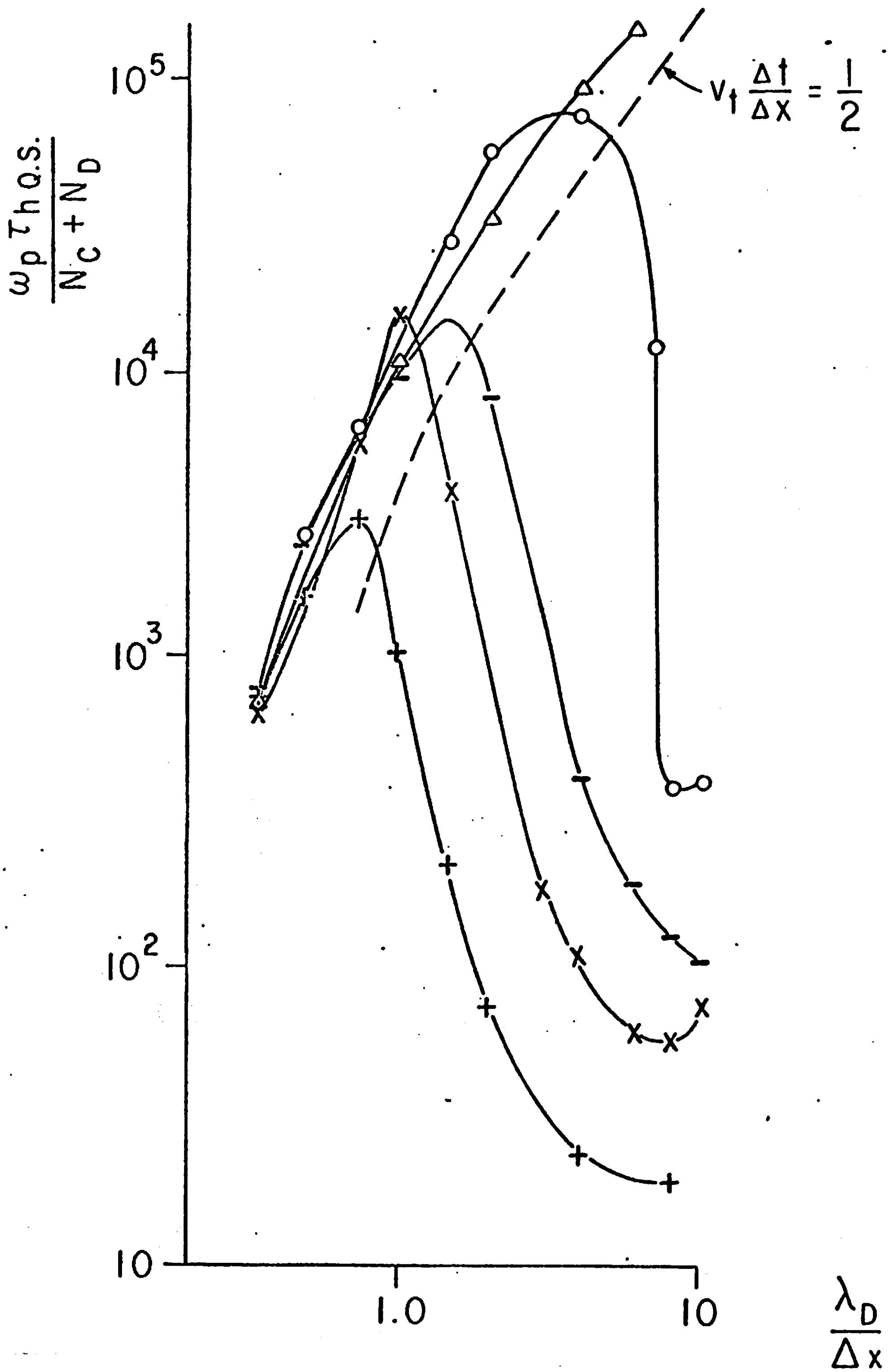

Fig. 6. Self-heating times divided by $N_C + N_D$ vs $\lambda_D/\Delta x$ for several $\omega_p \Delta t$ for QS

Symbol	Δ	O	—	×	+
	0.1	0.2	0.3	0.4	0.6

V COMPARISON OF SCHEMES; GAIN OF GOING TO A HIGHER ORDER ALGORITHM

As a comparison of the different algorithms studied, ratios of self-heating times of quadratic-spline to nearest-grid-point and cloud-in-cell to nearest grid point are plotted in Figs. 7, 8, and 9 for $\omega_p \Delta t = 0.1$, 0.2, 0.3, respectively. These figures indicate that CIC heating times are as much as 70 times longer than NGP and that QS is as much as 650 times longer than NGP.

These increases in heating times come at the expense of longer computation times. Actual measurements of cost of simulation per particle per time step on the CDC-7600 MFE computer at LLL show that $T \simeq 5, 11.6, 24$ μsec/particle/time step for NGP, CIC, and QS, respectively. Hence, we need a measure of accounting for this cost. We have chosen to define the gain of using a higher order weighting scheme as

$$\text{gain} \equiv \frac{\text{increase in self-heating time}}{\text{increase in computer time}} .$$

Going through the optimal path, we have gains as presented in Table I. Note that the gains of using higher order weightings, NGP $\rightarrow$ CIC, and CIC $\rightarrow$ QS are roughly one order of magnitude, much less than the gains in τ_h.

gain \ $\omega_p \Delta t$	0.1	0.2	0.3
CIC/NGP	$\frac{27.5}{2.3} = 11.9$	$\frac{48}{2.3} = 20.8$	$\frac{70}{2.3} = 30.4$
QS/NGP	$\frac{350}{4.8} = 72.9$	$\frac{650}{4.8} = 135.4$	$\frac{440}{4.8} = 91.6$
QS/CIC = (QS/NGP)/(CIC/NGP)	6.1	6.5	3.0

Table I Gain in going to a higher order algorithm. The ratios inside the table are increase in self-heating times (i.e., reduction in error in energy) over increase in cost (determined on the CDC 7600 MFE computer at LLL).

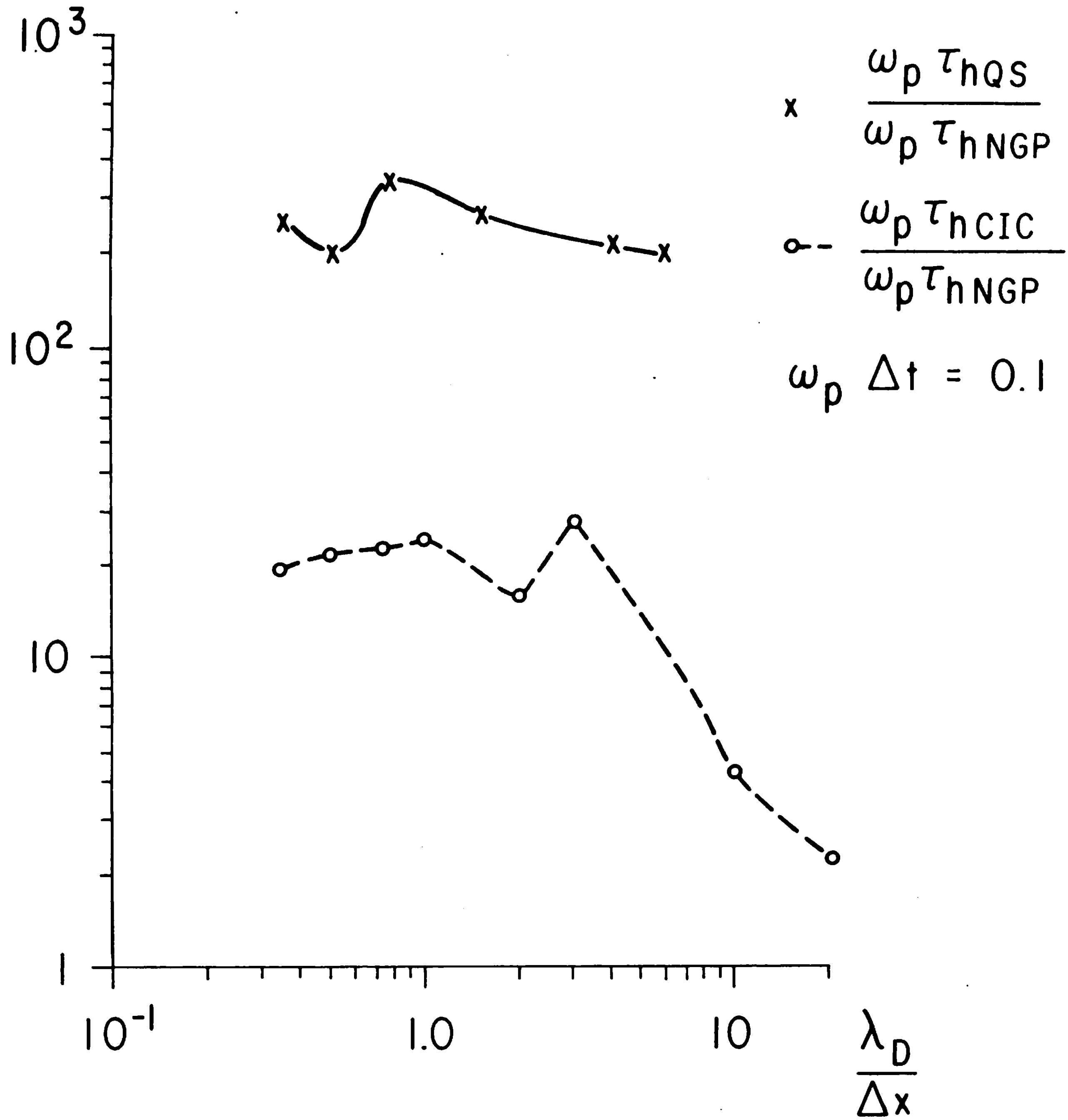

Fig. 7. Ratios of self-heating times vs $\frac{\lambda_D}{\Delta x}$ for $\omega_p \Delta t = 0.1$.

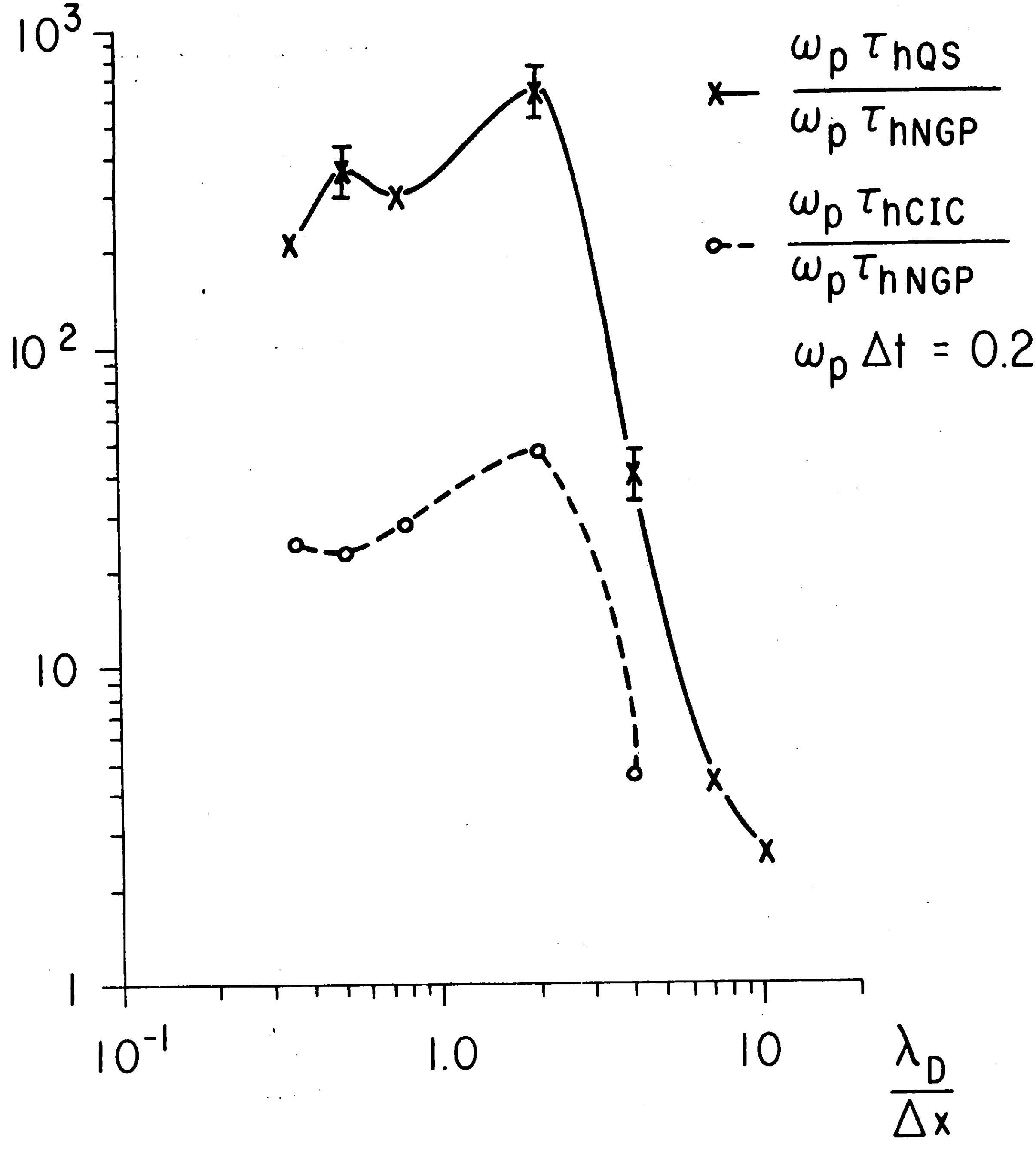

Fig. 8. Ratios of self-heating times vs $\frac{\lambda_D}{\Delta x}$ for $\omega_p \Delta t = 0.2$.

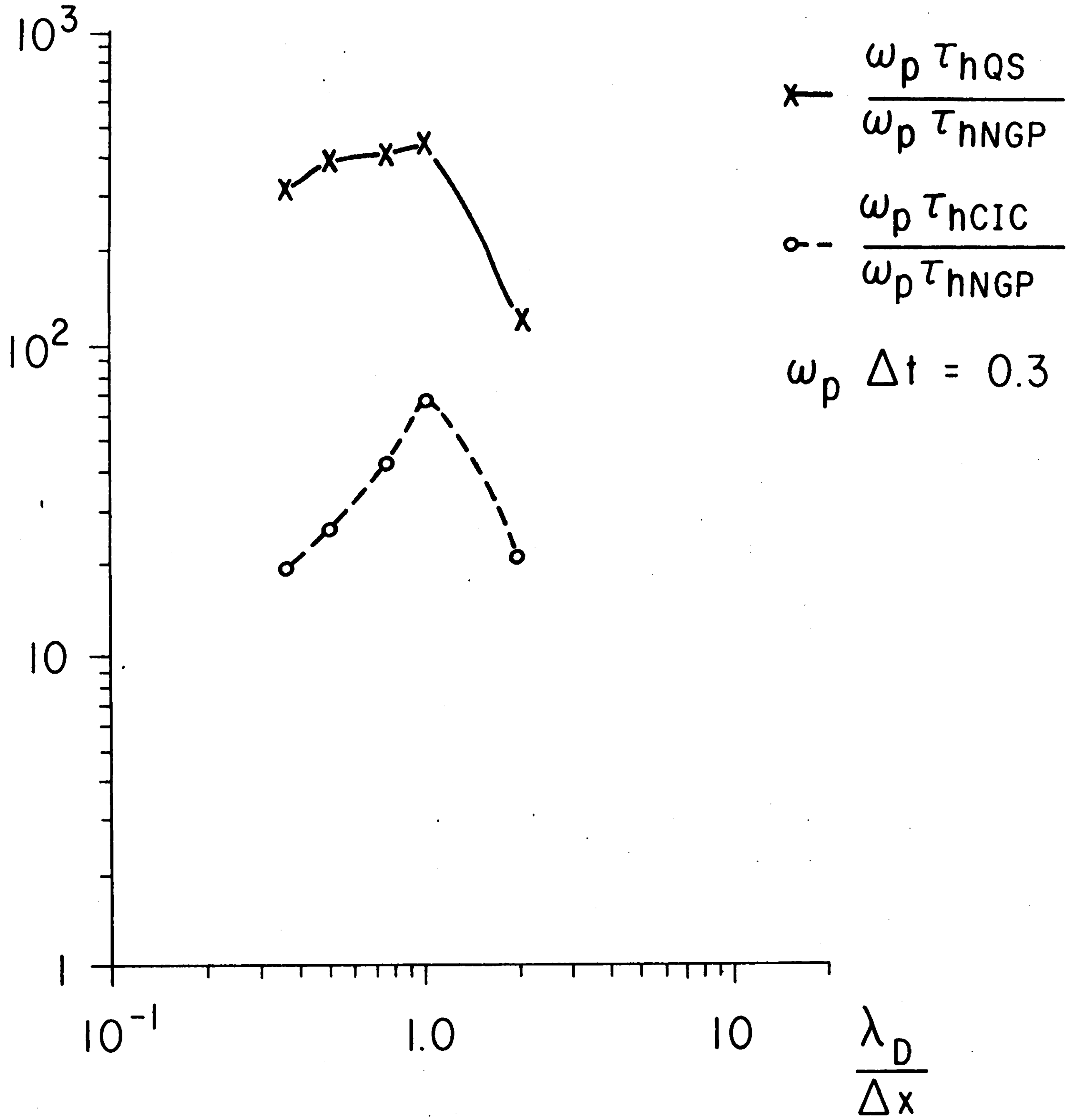

Fig. 9. Ratios of self-heating times vs $\frac{\lambda_D}{\Delta x}$ for $\omega_p \Delta t = 0.3$.

VI INCREASE IN GAIN DUE TO SMOOTHING

The self-heating time can be increased considerably by smoothing the charge density in k-space. The smoothing factor used was simple Fourier space truncation, where all the modes beyond k_{last} are dropped, as shown in Fig. 10. Fig. 11 shows the self-heating time $\omega_p \tau_h$ vs k_{max}/k_{last} for the different schemes used (keeping everything fixed but varying k_{last} for each scheme) (cases A70-A79, B63-B69, C43-C47). The gain in self-heating time due to k-space truncation is almost proportional to k_{max}/k_{last} for NGP and is close to but not quite proportional to $(k_{max}/k_{last})^2$ for CIC and $(k_{max}/k_{last})^3$ for QS. Thus, k-space truncation further increases the gain of CIC/NGP and QS/NGP and QS/CIC. Table II shows approximate gains with k-space truncation.

gain \ $\omega_{pe}\Delta t$	0.1	0.2	0.3
CIC/NGP $\times(k_{max}/k_{last})$	11.9	20.8	30.4
QS/NGP $\times(k_{max}/k_{last})^2$	72.9	135.4	91.6
QS/CIC $\times(k_{max}/k_{last})$	6.1	6.5	3.0

Table II. Gain with k-space truncation.

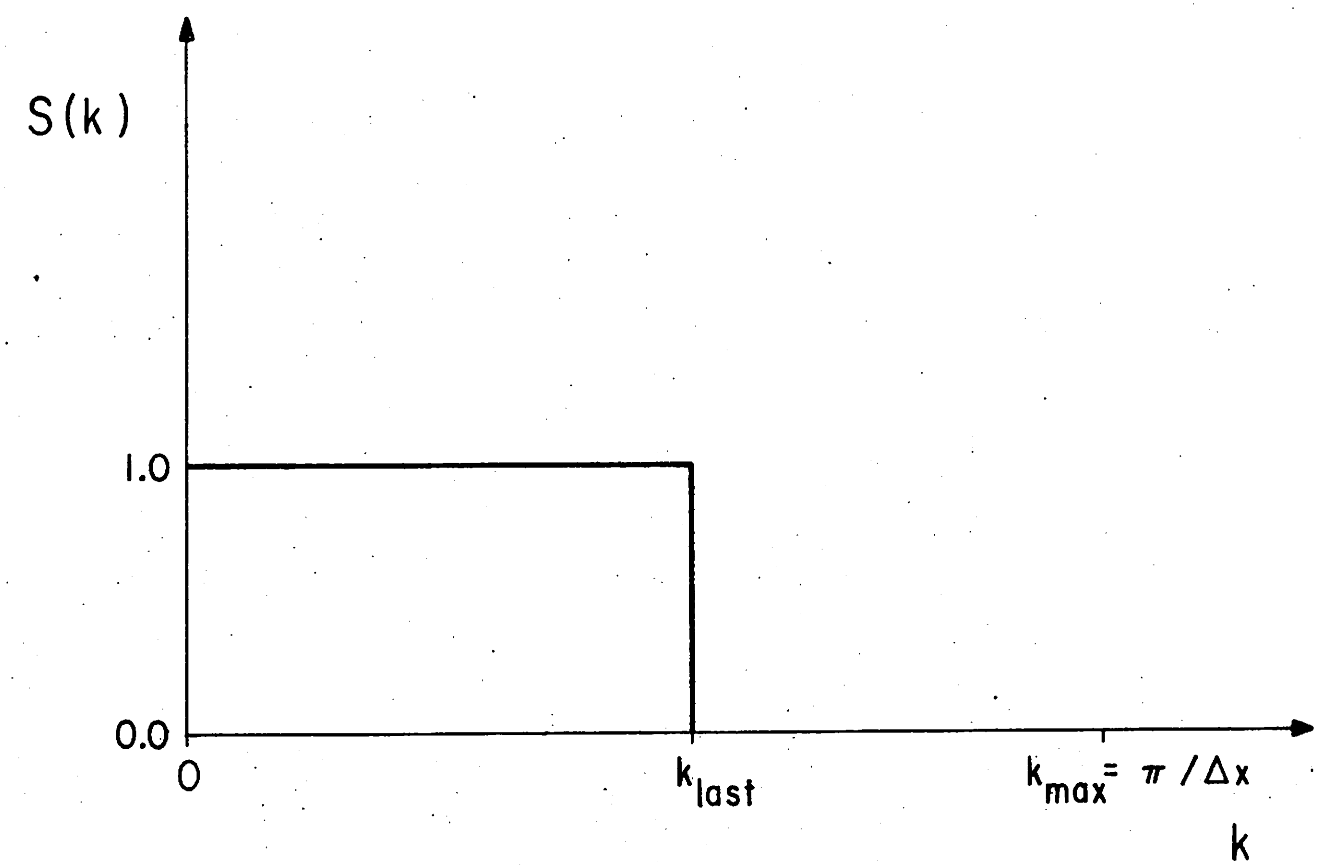

Fig. 10. Smoothing factor used in k-space truncation.

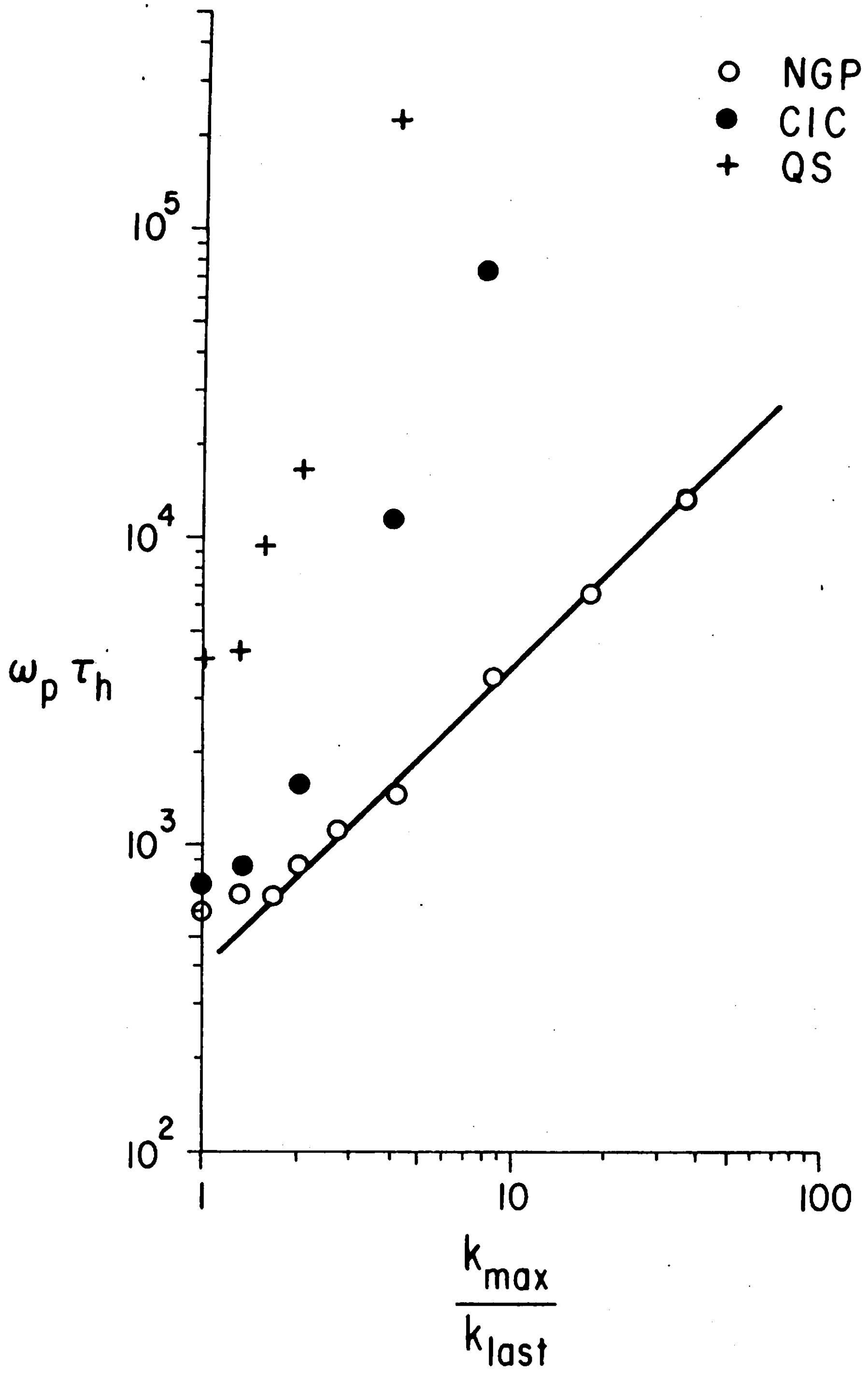

Fig. 11. Self-heating times vs k_{max}/k_{last} for NGP, CIC, QS.

VII CONCLUSIONS

The self-heating times are longest for $v_t \frac{\Delta t}{\Delta x} \approx \frac{3}{2}$ for NGP and $v_t \frac{\Delta t}{\Delta x} \approx \frac{1}{2}$ for CIC and QS. Roughly speaking, quadratic spline heating times are one order of magnitude longer than for cloud-in-cell, while cloud-in cell is one order of magnitude longer than nearest grid point, considering both gain in heating time and increase in cost. Smoothing by Fourier space truncation considerably increases the self-heating time and this increase is roughly proportional to

$$\left(\frac{k_{max}}{k_{last}}\right)^{n+1}$$

where n is the order of the weighting scheme, i.e., $n = 0$ for NGP, $n = 1$ for CIC, and $n=2$ for QS. Use of higher order algorithms is highly recommended, specially when k-space truncation is also used.

REFERENCES

1. C. K. Birdsall, A. B. Langdon, Plasma Physics via Computer Simulation, Part I, Chapter 3, University of California, Berkeley (Dec. 1975).
2. S. Gitomer, "Comments on Numerical Simulation of the Weibel Instability in One and Two Dimensions", Phys. Fluids 14, (Jul. 71) 1591-1592.
3. R. W. Hockney, "Measurements of Collisions and Heating Times in a Two-dimensional Thermal Plasma", J. Comp. Phys. 8, (Aug. 71) 19-44.
4. R. W. Hockney, S. P. Goel and J. W. Eastwood, "Quiet High Resolution Computer Models of a Plasma", J. Comp. Phys. 14, (Feb. 74) 148-158.
5. M. Abramowitz and I. A. Stegan, Handbook of Mathematical Functions, Applied Mathetmatics Series 55, (1964) 952-953.
6. J. Denavit, "Discrete Particle Effects in Whistler Simulation", J. Comp. Phys. 15 4 (Aug. 1974).
7. A. B. Langdon, "'Energy Conserving' Plasma Simulation Algorithms", J. Comp. Phys. 12 2 (Jun. 1973).
8. See Reference 1, Part II, Chapter 9.

APPENDIX A LOADING A THERMAL PLASMA WITH FIRST AND SECOND MOMENT CORRECTIONS

A one-dimensional Maxwellian velocity distribution,

$$f(v) = (2\pi)^{-\frac{1}{2}}\, v_t^{-1} \exp\left(\frac{-v^2}{2v_t^2}\right)$$

can be loaded using a set of random numbers $u_1, u_2, u_3, \dots, u_n$ to generate the velocity of one particle [5], i.e.

$$v_n(j) = v_t\left(\sum_{i=1}^{n} u_i - \frac{n}{2}\right) \Bigg/ \left(\frac{n}{12}\right)^{\frac{1}{2}} .$$

This process can be repeated for all the particles to be loaded; it requires calling n random numbers times the total number of particles. It produces better results as the number of particles in the system is increased $NP \to \infty$. The fluctuations about the desired distribution reduce as $NP^{\frac{1}{2}}$, which means that with a few hundred or thousand particles, the fluctuation level is of the order of a few percent, which may not be satisfactory.

The n^{th} moment of a Maxwellian distribution in 1d is

$$\begin{aligned}
\langle v^n \rangle &= \int_{-\infty}^{\infty} v^n e^{-v^2/2v_t^2}\, dv \Bigg/ \int_{-\infty}^{\infty} e^{-v^2/2v_t^2}\, dv \\
&= (\sqrt{2}\, v_t)^n \int_0^{\infty} x^{(n-1)/2} e^{-x}\, dx \Bigg/ \int_0^{\infty} x^{-\frac{1}{2}} e^{-x}\, dx \\
&= (\sqrt{2}\, v_t)^n\, \Gamma\left(\frac{n+1}{2}\right) \Big/ \Gamma(\tfrac{1}{2}) \quad . \qquad (1)
\end{aligned}$$

The expected values of the first five moments of a distribution with $v_t = 1$ and

$$\langle v^+ \rangle = - \langle v^- \rangle \equiv \int_0^\infty v e^{-v^2/2v_t^2} dv \Big/ \int_0^\infty e^{-v^2/2v_t^2} dv \tag{2}$$

are listed in Table I. Also listed are the ensemble averages over 10 separate loadings with a different set of random numbers used each time. We have used $n = 12$ and NP, the number of particles, equal to 1024. The higher moments are quite different from what is desired; the lower moments are within the expected fluctuation level of the random number generator, i.e., $\frac{\sqrt{N}}{N} = \frac{1}{\sqrt{2024}} = 0.03125$.

An improvement in all the odd moments can be achieved by loading a symmetric distribution, i.e.,

$$v_n(j) = \begin{cases} v_t \left[\sum_{i=1}^{n} u_i - \frac{n}{2} \right] \left(\frac{n}{12} \right)^{-\frac{1}{2}} & j = 1,2,\ldots, \frac{NP}{2} \\ -v_n(j - \frac{NP}{2}) & j = \frac{NP}{2} + 1, \frac{NP}{2} + 2, \ldots, NP \end{cases}$$

This method requires only half as many random numbers, $n \times \frac{NP}{2}$. Ensemble averages over 20 loadings of this distribution are listed in Table AI. Some improvement occurs. However, although the second moment averaged over 20 runs is only off by 2 per cent, the standard deviation of this moment about v_t^2 is $0.05\ v_t^2$.

	$\langle v \rangle$	$\langle v^2 \rangle$	$\langle v^3 \rangle$	$\langle v^4 \rangle$	$\langle v^5 \rangle$	$\langle v \rangle^+$	$\lvert\langle v \rangle^-\rvert$
expected value	0	1.0	0	3.0	0	0.3989	0.3989
nonsymmetric random loader	0.04	0.96	0.18	2.73	1.02	0.4210	0.3604
symmetric random loader	0	0.98	0	2.82	0	0.3879	0.3879

Table AI Several moments with $n = 12$, $NP = 1024$, $v_t = 1$.
1st row is the expected value from theory with no cutoff.
2nd row is the ensemble average over 10 separate loadings
3rd row is the ensemble average over 20 separate loadings.

A second improvement would be achieved if we could reduce this deviation to zero. This can be done by using a correction method suggested by Gitomer [2]. In this correction scheme, the particles are divided into ℓ groups of m particles. If a symmetric distribution has already been loaded, it is then best to correct each half of the distribution separately. Next one computes the mean and square means of the velocities of particles in each group $\bar{v}$, $\overline{v^2}$, by

$$\bar{v} = \frac{1}{m}\sum_{i=1}^{m} v_i \quad , \quad \overline{v^2} = \frac{1}{m}\sum_{i=1}^{m} v_i^2$$

then computes a correction factor ALPHA $= \left(v_t^2/(\overline{v^2} - \bar{v})^2\right)^{\frac{1}{2}}$ and next the corrected velocities

$$v_{i_{\text{corrected}}} = \text{ALPHA}(v_i - \bar{v}) \ .$$

It is important to be careful in the division of the particles into groups. For small values of m , we obtain an orderly and noiseless distribution but a poor Maxwellian. With $NP = 1024$ and $m = 2$, one gets two beams at $\pm v_t$. These distributions are sketched in Fig. A1; with $m = 4$, we get a distribution similar to a step function with cutoffs at $\pm 2.3\ v_t$. As m increases, the cutoff level goes up to $\pm 3\ v_t$ for $m = 32$ or higher. The measured values for the moments are given in Table AII and plotted in Fig. A2, showing rapid approach to Maxwellian values.

In the study of self-heating times, this improved version of the thermal loader was used with $\ell = 1$, where the resulting distribution was very nearly Maxwellian.

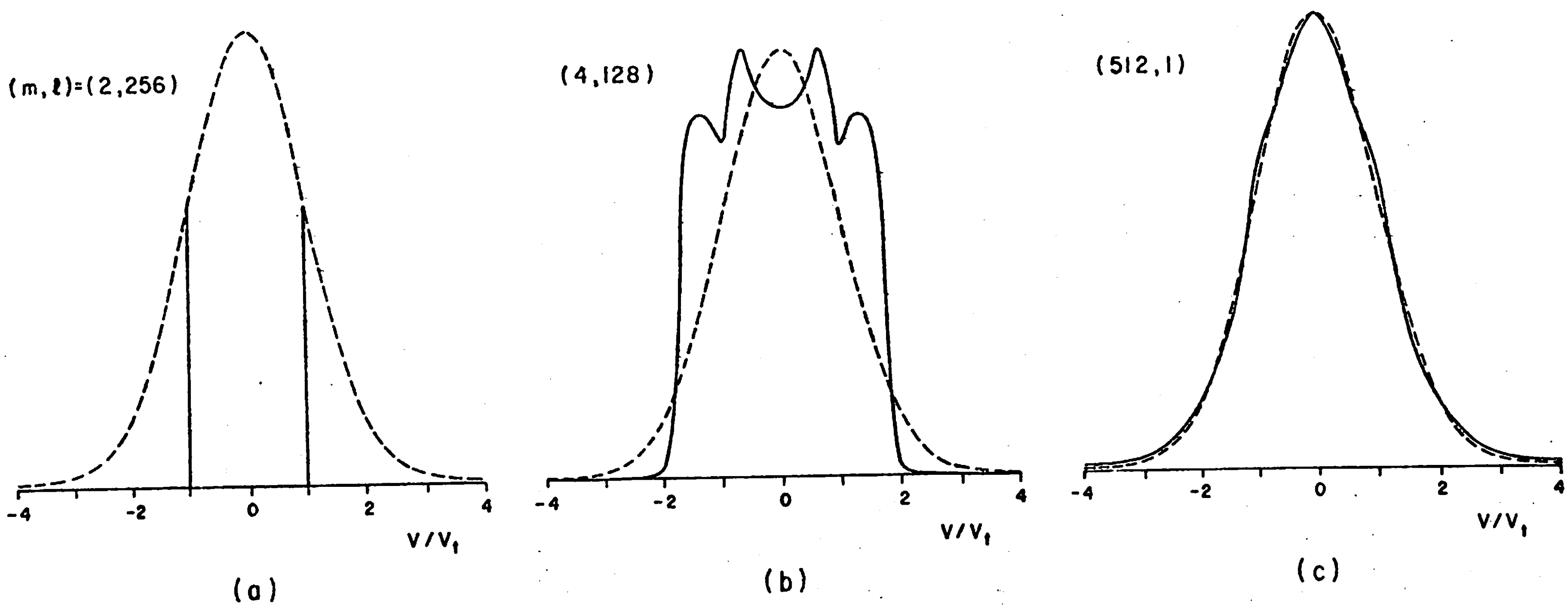

Fig. A1 Distribution functions with first and second moment correction as a function of m, the number of particles corrected in a group. ℓ is the total number of groups corrected. The solid line is drawn from silmulation with NP = 1024, with 31 bins in v. The dashed line is the Maxwellian for the same energy. The resulting distributions are (a) $m = 2$, producing two streams at $\pm v_t$, (b) $m = 4$, almost a square distribution, (c) $m = 512$, very nearly a Maxwellian.

m	$\langle v \rangle$	$\langle v^2 \rangle$	$\langle v^3 \rangle$	$\langle v^4 \rangle$	$\langle v^5 \rangle$	$\langle v \rangle^+ = -\langle v \rangle^-$
2	0	1.0	0	1	0	.500
4	0	1.0	0	1.838	0	.432
8	0	1.0	0	2.539	0	.411
16	0	1.0	0	2.686	0	.403
32	0	1.0	0	2.738	0	.399
64	0	1.0	0	2.790	0	.400
128	0	1.0	0	2.868	0	.399
256	0	1.0	0	2.920	0	.400
512	0	1.0	0	2.924	0	.399
Maxwellian	0	1.0	0	3	0	.3989

Table AII Moments using symmetric loading and Gitomer's corrector.

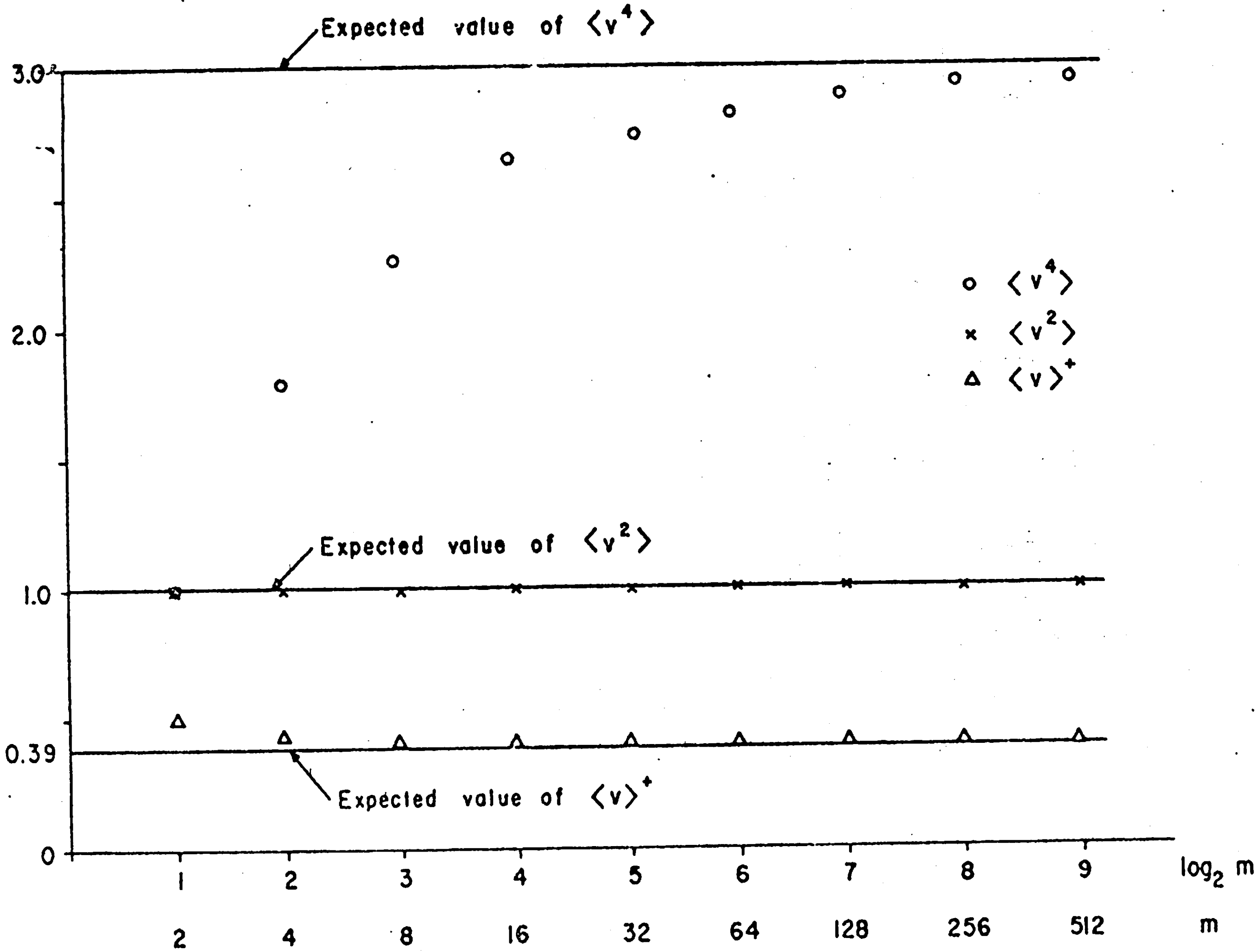

Fig. A2 Moments of distribution with first and second moment correction. m is the number of particles whose second moment was corrected in a group.

APPENDIX B QUADRATIC SPLINE WEIGHTING: APPLICATION TO ES1

Quadratic spline weighting algorithm [6], [7] has been placed in the plasma simulation code ES1 and as a check we present the dispersion for a cold plasma.

For momentum conserving codes. using quadratic splines, the shape factor $S(k)$ and the κ (from $\nabla\phi$) and K^2 (from $\nabla^2\phi$) operators are [8]

$$S(k) = \mathrm{dif}^3\left(\frac{k\Delta x}{2}\right) = \left[\frac{\sin(k\Delta x/2)}{k\Delta x/2}\right]^3 \tag{1}$$

$$\kappa(k) = k\ \mathrm{dif}\ (k\Delta x) = k\,\frac{\sin(k\Delta x)}{k\Delta x} \tag{2}$$

$$K^2(k) = k^2\mathrm{dif}^2\left(\frac{k\Delta x}{2}\right) = k^2\left[\frac{\sin(k\Delta x/2)}{k\Delta x/2}\right]^2 . \tag{3}$$

The dispersion equation for a cold plasma is, using $k_p \equiv k - pk_g$, $k_g \equiv \frac{2\pi}{\Delta x}$,

$$\frac{\omega^2}{\omega_p^2} = \frac{1}{K^2(k)} \sum_p k_p\ \kappa(k_p)\ S^2(k_p) . \tag{4}$$

Using Eqs. (1,2,3) in (4) we obtain

$$\frac{\omega^2}{\omega_p^2} = \frac{1}{k^2\mathrm{dif}(k\Delta x/2)} \sum_p k_p^2\ \mathrm{dif}(k_p\Delta x)\ \mathrm{dif}^6(k_p\Delta x/2) \tag{5}$$

$$= \frac{2^4\sin^4(k\Delta x/2)\ \sin(k\Delta x)}{\Delta x^5} \sum_p \frac{1}{k_p^{\ 5}} \tag{6}$$

$$= \left(\frac{2}{\Delta x}\right)^5 \sin^5(k\Delta x/2)\ \cos(k\Delta x/2) \sum_p \frac{1}{k_p^{\ 5}} . \tag{7}$$

Using the identity

$$\sum_p \frac{1}{(k - pk_g)^2} \equiv \left[\left(\frac{2}{\Delta x}\right)\sin(k\Delta x/2)\right]^{-2} \tag{8}$$

and differentiating three times successively, we get at each step

$$\sum_p \frac{1}{(k - pk_g)^3} = \cos(k\Delta x/2)\left[\left(\frac{2}{\Delta x}\right)\sin(k\Delta x/2)\right]^{-3} \qquad (9)$$

$$\sum_p \frac{1}{(k - pk_g)^4} = \frac{1}{3}\left(\frac{\Delta x}{2}\right)^2\left[\left(\frac{2}{\Delta x}\right)\sin(k\Delta x/2)\right]^{-2}$$

$$+ \cos^2(k\Delta x/2)\left[\left(\frac{2}{\Delta x}\right)\sin(k\Delta x/2)\right]^{-4} \qquad (10)$$

$$\sum_p \frac{1}{(k - pk_g)^5} = \cos(k\Delta x/2)\left[\left(\frac{2}{\Delta x}\right)\sin(k\Delta x/2)\right]^{-5}$$

$$\cdot\left[\frac{2}{3}\sin^2(k\Delta x/2) + \cos 2(k\Delta x/2)\right] \qquad (11)$$

$$\sum_p \frac{1}{k_p{}^5} = \cos(k\Delta x/2)\left[\left(\frac{2}{\Delta x}\right)\sin(k\Delta x/2)\right]^{-5}\left[\frac{2 + \cos^2(k\Delta x/2)}{3}\right]. \qquad (12)$$

Thus, the dispersion equation reduces to

$$\frac{\omega^2}{\omega_p{}^2} = \cos^2(k\Delta x/2)\left(\frac{2 + \cos^2(k\Delta x/2)}{3}\right). \qquad (13)$$

The quadratic spline weighting algorithm has been tested out in our electrostatic one-dimensional code ES1; the cold plasma results along with the theory are plotted in Fig. B1. The parameters of the run are as given in Table BI below.

L = 6.28	NP = 128
Δt = 0.2	ω_p = 1.0
NG = 64	x1 = 0.001

Table BI Parameters used for measurement of cold plasma dispersion using quadratic spline weighting.

The results show very good agreement with theory. This algorithm was used in our study of self-heating times with second order weighting.

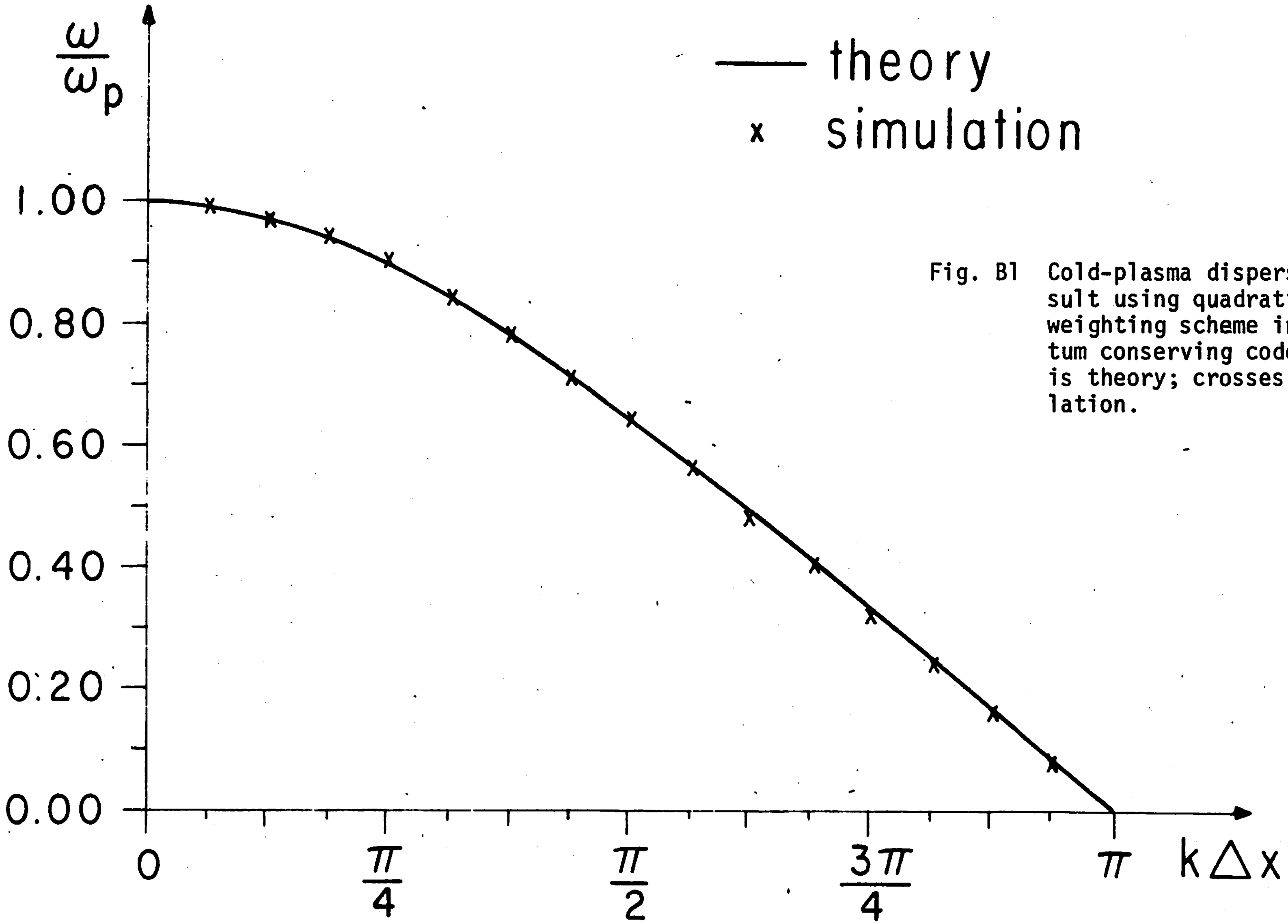

Fig. B1 Cold-plasma dispersion result using quadratic spline weighting scheme in a momentum conserving code. Line is theory; crosses are simulation.

Table C1 NEAREST GRID POINT

Case No.	L	NG	NP	Δx	Δt	ω_p	v_t	$\omega_p\Delta t$	$\lambda_D/\Delta x$	N_C	N_D	N_C+N_D	k_{max}/k_{last}	$\omega_p\tau_h$	$\omega_p\tau_h/N_C+N_D$
A1	64	64	1024	1.0	1.0	0.1	0.1	0.10	1.0	16	16	32	1.0	1296.00	[illegible]
A2	64	64	1024	1.0	1.4	0.1	0.1	0.14	1.0	16	16	32	1.0	1207.5	37.73
A3	64	64	1024	1.0	4.0	0.1	0.1	0.40	1.0	16	16	32	1.0	[illegible]	19.53
A4	64	64	1024	1.0	6.0	0.1	0.1	0.60	1.0	16	16	32	1.0	382.00	11.93
A5	64	64	1024	1.0	10.0	0.1	0.1	1.00	1.0	16	16	32	1.0	150.00	4.68
A6	64	64	1024	1.0	14.0	0.1	0.1	1.40	1.0	16	16	32	1.0	70.00	2.18
A7	64	64	64	1.0	0.2	0.4	0.4	0.08	1.0	1	1	2	1.0	74	31
A8	64	64	128	1.0	0.2	0.4	0.4	0.08	1.0	2	2	4	1.0	115	[illegible]
A9	64	64	256	1.0	0.2	0.4	0.4	0.08	1.0	4	4	8	1.0	160	20
A10	64	64	512	1.0	0.2	0.4	0.4	0.08	1.0	8	8	16	1.0	360	22.5
A11	64	64	1024	1.0	0.2	0.4	0.4	0.08	1.0	16	16	32	1.0	[illegible]	18.75
A12	64	64	1024	1.0	0.2	1.0	0.5	0.2	0.5	16	8	24	1.0	150	6.25
A13	128	32	512	4.0	1	0.2	0.4	0.2	0.5	16	8	24	1.0	159	6.625
A14	64	32	1024	2.0	2	0.1	0.1	0.2	0.5	32	16	48	1.0	323	6.729
A15	64	64	256	1.0	0.2	1.0	0.5	0.2	0.5	4	2	6	1.0	37.5	6.25
~~A16~~	~~64~~	~~64~~	~~1024~~	~~1~~	~~0.1~~	~~1.0~~	~~0.35~~	~~0.1~~							
A16 ~~A17, A21~~	32	32	256	1.0	0.1	1.0	0.35	0.1	0.35	8	2.8	10.8	1.0	37	3.43
A17	64	64	1024	1.0	0.1	1.0	0.5	0.1	0.5	16	8	24	1.0	199	8.29
A18	32	32	256	1.0	0.1	1.0	0.75	0.1	0.75	8	6	14	1.0	335	23.93
A19	32	32	256	1.0	0.1	1.0	4	0.1	4	8	32	40	1.0	17100	427.5
A20	32	32	256	1.0	0.1	1.0	10	0.1	10	8	80	88	1.0	[illegible]	1020
A21	32	32	256	1.0	0.1	1.0	20	0.1	20	8	160	168	1.0	155000 [illegible]	922.62 [illegible]
A22	64	8	1024	8.0	2	0.1	0.1	0.2	0.125	128	16	144	1.0	20	.138
A23	64	16	1024	4.0	2	0.1	0.1	0.2	0.25	64	16	80	1.0	97.5	1.218
A24	32	32	256	1.0	0.2	1.0	0.35	0.2	0.35	8	2.8	10.8	1.0	35	3.24
~~A25~~	~~64~~	~~64~~	~~256~~	~~1.0~~	~~0.05~~										
A25	32	32	256	1.0	0.2	1.0	0.75	0.2	0.75	8	6	14	1.0	300	21.43
A26	64	64	1024	1.0	2	0.1	0.1	0.2	1.0	16	16	32	1.0	1070	[illegible]
A27	32	32	512	1.0	1	0.2	0.4	0.2	[illegible]	16	32	48	1.0	3972.	82.75
A28	64	128	1024	0.5	2	0.1	0.1	0.2	2	8	16	24	1.0	[illegible]	[illegible]

(Table C1 cont. ...)

Case No.	L	NG	NP	Δx	Δt	ω_p	v_t	$\omega_p \Delta t$	$\lambda_D/\Delta x$	N_C	N_D	N_C+N_D	k_{max}/k_{last}	$\omega_p \tau_h$	$\omega_p \tau_h / N_C+N_D$
A60	32	32	256	1	0.6	1.0	2.0	0.6	2	8.0	16.0	24.0	1.0	420	17.5
A61	32	32	256	1	0.6	1.0	4.0	0.6	4	8.0	32.0	40.0	1.0	660	16.5
A62	32	32	256	1	0.6	1.0	6.0	0.6	6	8.0	48.0	56.0	1.0	980	17.5
A63	32	32	256	1	0.6	1.0	8.0	0.6	8	8.0	64.0	72.0	1.0	1046	14.5
A64	32	32	256	1	0.5	1.5	1.0	0.75	1.66	8.0	5.3	13.3	1.0	105	7.87
A65	64	64	1024	1	8	0.1	0.1	0.8	1	16.0	16.0	32.0	1.0	250	7.81
~~A65~~	~~64~~	~~64~~	~~1024~~	~~1~~	~~10~~	~~0.1~~	~~0.1~~	~~1.0~~	~~1~~	~~16~~	~~16~~	~~32~~	~~1~~	~~150~~	[illegible]
A66	64	64	1024	1	12	0.1	0.1	1.2	1	16.0	16.0	32.0	1.0	85	2.65
A67	64	64	1024	1	0.01	1	0.5	0.01	0.5	16.0	8.0	24.0	1.0	174	7.25
A68	64	64	1024	1	0.5	0.1	0.1	0.05	1	16.0	16.0	32.0	1.0	1412	44.12
A69	64	64	256	1	0.05	1	0.5	0.05	0.5	4.0	2.0	6.0	1.0	56	9.33
A70	64	64	1024	1	0.05	1	0.5	0.05	0.5	16.0	8.0	24.0	1.0	202	8.41
A71	64	64	256	1	0.2	1	0.5	0.2	0.5	4.0	2.0	6.0	2.0	55	9.16
A72	64	256	512	0.25	1	0.2	0.1	0.2	2	2.0	4.0	6.0	8.0	3290	548.33
A73	64	256	512	0.25	1	0.2	0.1	0.2	2	2.0	4.0	6.0	2.0	772	128.66
A74	64	256	512	0.25	1	0.2	0.1	0.2	2	2.0	4.0	6.0	16	7044	1174
A75	64	256	512	0.25	1	0.2	0.1	0.2	2	2.0	4.0	6.0	32	13460	2243.33
~~A75~~	~~64~~	~~256~~	~~512~~	~~0.25~~	~~1~~	~~0.2~~	~~0.1~~	~~0.2~~	~~2~~	~~2~~	~~4~~	~~6~~			
A76	320	256	512	1.25	1	0.2	0.1	0.2	0.4	2.0	0.8	2.8	8	108	38.57
A77	192	256	512	0.75	1	0.2	0.1	0.2	0.66	2.0	1.33	3.33	8	282	84.68
A78	256	256	512	1	1	0.2	0.1	0.2	0.5	2.0	1.0	3.0	8	150	50
A79	128	256	512	0.5	1	0.2	0.1	0.2	1.0	2.0	2.0	4.0	8	764	191

(Table C1 cont. ...)

	L	NG	NP	Δx	Δt	ω_p	v_t	$\omega_p \Delta t$	$\lambda_D/\Delta x$	N_C	N_D	N_C+N_D	k_{max}/k_{last}	$\omega_p \tau_h$	$\omega_p \tau_h / N_C+N_D$
A29	64	256	1024	.25	2	0.1	0.1	0.2	4	4	16	20	1.0	3450	172.5
A30	32	32	256	1.0	0.2	1.0	7	0.2	7	8	56	64	1.0	17575	275
A31	32	32	256	1.0	0.2	1.0	10	0.2	10	8	80	88	1.0	14250	162
A32	32	32	256	1.0	0.3	1.0	0.35	0.3	0.35	8	2.8	10.8	1.0	30	2.78
A33	32	32	256	1.0	0.3	1.0	0.5	0.3	0.5	8	4	12	1.0	75	6.25
A34	32	32	256	1.0	0.3	1.0	0.75	0.3	0.75	8	6	14	1.0	182	13
A35	32	32	256	1.0	0.3	1.0	1.0	0.3	1.0	8	8	16	1.0	330	20.625
A36	32	32	256	1.0	0.3	1.0	1.5	0.3	1.5	8	12	20	1.0	765	38.25
A37	32	32	256	1.0	0.3	1.0	2	0.3	2	8	16	24	1.0	1535	63.95
A38	32	32	256	1.0	0.4	1.0	0.35	0.4	0.35	8	2.8	10.8	1.0	27	2.5
A39	32	32	256	1.0	0.4	1.0	0.5	0.4	0.5	8	4	12	1.0	78	6.5
A40	32	32	256	1.0	0.4	1.0	0.75	0.4	0.75	8	6	14	1.0	197	14.07
A41	32	32	256	1.0	0.4	1.0	1.0	0.4	1.0	8	8	16	1.0	340	21.25
A42	32	32	256	1.0	0.4	1.0	1.5	0.4	1.5	8	12	20	1.0	685	34.25
A43	32	32	256	1.0	0.4	1.0	2	0.4	2	8	16	24	1.0	970	40.41
A44	32	32	256	1.0	0.4	1.0	4	0.4	4	8	32	40	1.0	1920	48
A45	32	32	256	1.0	0.4	1.0	6	0.4	6	8	48	56	1.0	2910	51.96
A46	32	32	256	1.0	0.4	1.0	8	0.4	8	8	64	72	1.0	2805	38.95
A47	32	32	256	1.0	0.4	1.0	10	0.4	10	8	80	88	1.0	2195	24.9
A48	32	32	256	1.0	0.5	1.0	0.35	0.5	0.35	8	2.8	10.8	1.0	30	2.78
A49	32	32	256	1.0	0.5	1.0	0.5	0.5	0.5	8	4	12	1.0	56	4.67
A50	32	32	256	1.0	0.5	1.0	0.75	0.5	0.75	8	6	14	1.0	180	12.86
A51	32	32	256	1.0	0.5	1.0	1.0	0.5	1.0	8	8	16	1.0	425	26.56
A52	32	32	256	1.0	0.5	1.0	1.5	0.5	1.5	8	12	20	1.0	455	22.75
A53	32	32	256	1.0	0.5	1.0	2.0	0.5	2	8	16	24	1.0	570	23.75
A54	32	32	256	1.0	0.5	1.0	4	0.5	4	8	32	40	1.0	840	21
A55	32	32	256	1.0	0.5	1.0	10	0.5	10	8	80	88	1.0	1628	18.5
A56	32	32	256	1.0	0.6	1.0	0.35	0.6	0.35	8	2.8	10.8	1.0	24	2.22
A57	32	32	256	1.0	0.6	1.0	0.5	0.6	0.5	8	4	12	1.0	44	3.66
A58	32	32	256	1.0	0.6	1.0	0.75	0.6	0.75	8	6	14	1.0	140	10
A59	32	32	256	1.0	0.6	1.0	1.0	0.6	1.0	8	8	16	1.0	220	13.75

Table C2 CLOUD-IN-CELL

Case No.	L	NG	NP	Δx	Δt	ω_p	t	$\omega_p \Delta t$	$\lambda_D/\Delta x$	N_C	N_D	N_C+N_D	k_{max}/k_{last}	$\omega_p \tau_h$	$\omega_p \tau_h / (N_C+N_D)$
B1	64	64	64	1.0	0.2	0.4	0.4	0.08	1.0	1	1	2	1.0	2200	1100
B2	64	64	128	1.0	0.2	0.4	0.4	0.08	1.0	2	2	4	1.0	3400	850
B3	64	64	256	1.0	0.2	0.4	0.4	0.08	1.0	4	4	8	1.0	[illegible]	875
B4	64	64	512	1.0	0.2	0.4	0.4	0.08	1.0	8	8	16	1.0	13500	843.75
B5	64	64	1024	1.0	0.2	0.4	0.4	0.08	1.0	16	16	32	1.0	26500	828.12
B6	32	32	256	1.0	0.1	1.0	0.35	0.1	0.35	8	2.8	10.8	1.0	708	65.56
B7	64	64	1024	1.0	0.1	1.0	0.5	0.1	0.5	16	8	24	1.0	4320	180
B8	32	32	256	1.0	0.1	1.0	0.75	0.1	0.75	8	6	14	1.0	7590	542.14
B9	32	32	256	1.0	0.1	1.0	1.5	0.1	1.5	8	12	20	1.0	40000	2000
B10	32	32	256	1.0	0.1	1.0	3	0.1	3	8	24	32	1.0	[illegible]	7776
B11	32	32	256	1.0	0.1	1.0	10	0.1	10	8	80	88	1.0	385,000 ± 25,000	4375 ± 285
B12	32	32	256	1.0	0.1	1.0	20	0.1	20	8	160	168	1.0	360,000 ± 16,000	2142 ± 60
B13	32	32	256	1.0	0.2	1.0	0.35	0.2	0.35	8	2.8	10.8	1.0	865	80.09
B14	64	64	256	1.0	0.2	1.0	0.5	0.2	0.5	4	2	6	1.0	890	148.33
B15	32	32	256	1.0	0.2	1.0	0.5	0.2	0.5	8	4	12	1.0	1720	143.33
B16	64	64	1024	1.0	0.2	1.0	0.5	0.2	0.5	16	8	24	1.0	4235	176.45
B17	128	32	512	4.0	1.0	0.2	0.4	0.2	0.5	16	8	24	1.0	4680	195
B18	96	32	512	3.0	1.0	0.2	0.4	0.2	0.66	16	10.66	26.66	1.0	8587	322.09
B19	32	32	256	1.0	0.2	1.0	0.75	0.2	0.75	8	6	14	1.0	8475	605.35
B20	64	32	512	2.0	1.0	0.2	0.4	0.2	1.0	16	16	32	1.0	42425	1325
B21	32	32	256	1.0	0.2	1.0	1.5	0.2	1.5	~~16~~ 8	12	20	1.0	67600	3380
B22	32	32	256	1.0	0.2	1.0	2.0	0.2	2.0	~~16~~ 8	16	24	1.0	96400	4016.6
B23	32	32	256	1.0	0.2	1.0	3.0	0.2	3.0	~~16~~ 8	24	32	1.0	53000	1325
B24	32	32	256	1.0	0.2	1.0	4.0	0.2	4.0	8	32	40	1.0	195000	5468.75
B25	32	32	256	1.0	0.2	1.0	8.0	0.2	8.0	~~16~~ 8	64	72	1.0	24855	345.2
B26	32	32	256	1.0	0.3	1.0	0.35	0.3	0.35	8	2.8	10.8	1.0	575	53.24
B27	64	64	1024	1.0	0.3	1.0	0.5	0.3	0.5	16	8	24	1.0	4650	193.75
B28	32	32	256	1.0	0.3	1.0	0.5	0.3	0.5	8	4	12	1.0	2000	166.67
B29	32	32	256	1.0	0.3	1.0	0.75	0.3	0.75	8	6	14	1.0	7880	562.85
B30	32	32	256	1.0	0.3	1.0	1.0	0.3	1.0	8	8	16	1.0	22985	1436.5
B31	32	32	256	1.0	0.3	1.0	2.0	0.3	2.0	8	16	24	1.0	33275	1386.4
B32	32	32	256	1.0	0.3	1.0	4.0	0.3	4.0	8	32	40	1.0	9815	245.38

(Table C2 cont. ...)

Case No.	L	NG	NP	Δx	Δt	ω_p	t	$\omega_p \Delta t$	$\lambda_D/\Delta x$	N_C	N_D	N_C+N_D	k_{max}/k_{last}	$\omega_p \tau_h$	$\omega_p \tau_h / N_C+N_D$
B33	32	32	256	1.0	0.3	1.0	6.0	0.3	6	8	48	56	1.0	8502	151.82
B34	32	32	256	1.0	0.3	1.0	8.0	0.3	8	8	64	72	1.0	7758	107.75
B35	32	32	256	1.0	0.3	1.0	10.0	0.3	10	8	80	88	1.0	6750	76.7
B36	32	32	256	1.0	0.4	1.0	0.35	0.4	0.35	8	2.8	10.8	1.0	1023	94.72
B37	16	32	128	0.5	0.4	1.0	0.25	0.4	0.5	4	2	6	1.0	1135	189.16
B38	32	32	256	1.0	0.4	1.0	0.5	0.4	0.5	8	4	12	1.0	2295	191.25
B39	64	64	1024	1.0	0.4	1.0	0.5	0.4	0.5	16	8	24	1.0	4160	173.33
B40	64	64	256	1.0	0.4	1.0	0.5	0.4	0.5	4	2	6	1.0	1150	191.66
B41	32	32	256	1.0	0.4	1.0	0.75	0.4	0.75	8	6	14	1.0	5860	418.57
B42	16	32	128	0.5	0.4	1.0	0.5	0.4	1.0	4	4	8	1.0	7120	890
B43	32	32	256	1.0	0.4	1.0	1.5	0.4	1.5	8	12	20	1.0	13080	654
B44	32	32	256	1.0	0.4	1.0	2.0	0.4	2	8	16	24	1.0	10200	425
B45	32	32	256	1.0	0.4	1.0	4.0	0.4	4	8	32	40	1.0	2985	74.63
B46	16	32	128	0.5	0.4	1.0	6.0	0.4	6	4	24	28	1.0	1800	64.24
B47	16	32	128	0.5	0.4	1.0	8.0	0.4	8	4	32	36	1.0	1705	47.36
B48	32	32	256	1.0	0.5	1.0	0.35	0.5	0.35	8	2.8	10.8	1.0	965	89.35
B49	32	32	256	1.0	0.5	1.0	0.5	0.5	0.5	8	4	12	1.0	2230	185.83
B50	32	32	256	1.0	0.5	1.0	0.75	0.5	0.75	8	6	14	1.0	5400	385.71
B51	32	32	256	1.0	0.5	1.0	1.0	0.5	1	8	8	16	1.0	9830	614.38
B52	32	32	256	1.0	0.5	1.0	2.0	0.5	2	8	16	24	1.0	3530	147.08
B53	32	32	256	1.0	0.5	1.0	4.0	0.5	4	8	32	40	1.0	1622	40.55
B54	32	32	256	1.0	0.5	1.0	8.0	0.5	8	8	64	72	1.0	1515	21.04
B55	32	32	256	1.0	0.5	1.0	10.0	0.5	10	8	80	88	1.0	1784	20.27
B56	32	32	256	1.0	0.6	1.0	0.35	0.6	0.35	8	2.8	10.8	1.0	805	74.54
B57	64	64	256	1.0	0.6	1.0	0.5	0.6	0.5	4	2	6	1.0	1385	230.83
B58	64	64	1024	1.0	0.6	1.0	0.5	0.6	0.5	16	8	24	1.0	4650	193.75
B59	32	32	256	1.0	0.6	1.0	0.75	0.6	0.75	8	6	14	1.0	4450	317.86
B60	32	32	256	1.0	0.6	1.0	1.0	0.6	1.0	8	8	16	1.0	6360	397.5
B61	64	64	1024	1.0	.01	1.0	0.1	0.01	0.1	16	1.6	17.6	1.0	4584	260.45
B62	64	64	1024	1.0	1.0	0.8	0.8	0.8	1.0	16	16	32	1.0	2056	64.25
B63	64	64	1024	1.0	1.0	1.2	1.2	1.2	1.0	16	16	32	1.0	222	6.93
B64	128	128	256	1.0	1.0	0.2	0.1	0.2	0.5	2	1	3	1.33	596	198.66
B65	128	128	256	1.0	1.0	0.2	0.1	0.2	0.5	2	1	3	2.0	1400	466.66
B66	128	128	256	1.0	1.0	0.2	0.1	0.2	0.5	2	1	3.	4.0	9524	3174.66
B67	128	128	256	1.0	1.0	0.2	0.1	0.2	0.5	2	1	3	32.0	136000	4533.33
B68	64	64	256	1.0	0.2	1.0	0.5	0.2	0.5	4	2	6	2.0	2640	440
B69	64	64	256	1.0	0.1	1.0	0.5	0.1	0.5	4	2	6	2.0	2532	422

Table C3 QUADRATIC SPLINE

Case No.	L	NG	NP	Δx	Δt	ω_p	V_t	$\omega_p \Delta t$	$\lambda_D/\Delta x$	N_C	N_D	N_C+N_D	k_{max}/k_{last}	$\omega_p \tau_h$	$\omega_p \tau_h / N_C+N_D$
C1	32	32	256	1.0	0.1	1.0	0.35	0.1	0.35	8.0	2.88	10.88	1.0	9500	873
C2	32	32	256	1.0	0.1	1.0	0.50	0.1	0.50	8.0	4.00	12.00	1.0	20100	1676
C3	32	32	256	1.0	0.1	1.0	0.75	0.1	0.75	8.0	6.00	14.00	1.0	115500	8250
C4	32	32	256	1.0	0.1	1.0	1.00	0.1	1.00	8.0	8.00	16.00	1.0	175000 ± 10000	10937 ± 625
C5	32	32	256	1.0	0.1	1.0	2.00	0.1	2.00	8.0	16.00	24.00	1.0	775000 ± 25000	32290 ± 1041
C6	32	32	256	1.0	0.1	1.0	4.00	0.1	4.00	8.0	32.00	40.00	1.0	3,000,000 ± 100,000	75,000 ± 2500
C7	32	32	256	1.0	0.1	1.0	6.00	0.1	6.00	8.0	48.00	56.00	1.0	764,000 ± 100,000	13600 ± 1785
C8	32	32	256	1.0	0.2	1.0	0.35	0.2	0.35	8.0	2.88	10.88	1.0	7320	677.77
C9	32	32	256	1.0	0.2	1.0	0.50	0.2	0.50	8.0	4.00	12.00	1.0	32280	2690
C10	32	32	256	1.0	0.2	1.0	0.75	0.2	0.75	8.0	6.00	14.00	1.0	90000 ± 1000	6428 ± 71
C11	32	32	256	1.0	0.2	1.0	1.50	0.2	1.50	8.0	12.00	20.00	1.0	540,000 ± 20000	27000 ± 1000
C12	32	32	256	1.0	0.2	1.0	2.00	0.2	2.00	8.00	16.00	24.00	1.0	1,300,000 ± 150,000	54166 ± 6250
C13	32	32	256	1.0	0.2	1.0	4.00	0.2	4.00	8.00	32.00	40.00	1.0	275000 ± 20,000	6875 ± 500
C14	32	32	256	1.0	0.2	1.0	6.00	0.2	6.00	8.00	48.00	56.00	1.0	90,000	1607.14
C15	32	32	256	1.0	0.2	1.0	7.00	0.2	7.00	8.00	56.00	64.00	1.0	95000 ± 5000	1172 ± 80
C16	32	32	256	1.0	0.2	1.0	8.00	0.2	8.00	8.00	64.00	72.00	1.0	29000 ± 1000	402.78 ± 13.89
C17	32	32	256	1.0	0.2	1.0	10.00	0.2	10.00	8.00	80.00	88.00	1.0	37000	420
C18	32	32	256	1.0	0.3	1.0	0.35	0.3	0.35	8.00	2.88	10.88	1.0	9700	890
C19	32	32	256	1.0	0.3	1.0	0.50	0.3	0.50	8.00	4.00	12.00	1.0	30,000	2500
C20	32	32	256	1.0	0.3	1.0	0.75	0.3	0.75	8.00	6.00	14.00	1.0	75000	5357
C21	32	32	256	1.0	0.3	1.0	1.00	0.3	1.00	8.00	8.00	16.00	1.0	150000 ± 10000	9375 ± 625
C22	32	32	256	1.0	0.3	1.0	2.00	0.3	2.00	8.00	16.00	24.00	1.0	187,000	7791
C23	32	32	256	1.0	0.3	1.0	4.00	0.3	4.00	8.00	32.00	40.00	1.0	17300	432.5
C24	32	32	256	1.0	0.3	1.0	6.00	0.3	6.00	8.00	48.00	56.00	1.0	10500	187.5
C25	32	32	256	1.0	0.3	1.0	8.00	0.3	8.00	8.00	64.00	72.00	1.0	9155	127.15
C26	32	32	256	1.0	0.3	1.0	10.00	0.3	10.00	8.00	80.00	88.00	1.0	9000	102.27
C27	32	32	256	1.0	0.4	1.0	0.75	0.4	0.75	8.00	6.00	14.00	1.0	79000	5642
C28	32	32	256	1.0	0.4	1.0	1.00	0.4	1.00	8.0	8.0	16.00	1.0	240,000	15000
C29	32	32	256	1.0	0.4	1.0	1.50	0.4	1.50	8.0	12.0	20.0	1.0	76320	3816
C30	32	32	256	1.0	0.4	1.0	3.0	0.4	3.0	8.0	24.00	32.0	1.0	5880	183.75
C31	32	32	256	1.0	0.4	1.0	4.0	0.4	4.0	8.0	32.00	40.0	1.0	4440	111
C32	32	32	256	1.0	0.4	1.0	6.0	0.4	6.0	8.0	48.00	56.00	1.0	3310	59.1
C33	32	32	256	1.0	0.4	1.0	8.0	0.4	8.0	8.0	64.0	72.0	1.0	4100 ± 700	57 ± 9.6
C34	32	32	256	1.0	0.4	1.0	10.00	0.4	10.00	8.0	80.0	88.0	1.0	6400 ± 800	72.72 ± 9.09
C35	32	32	256	1.0	0.6	1.0	0.35	0.6	0.35	8.0	2.88	10.88	1.0	9000	833.33
C36	32	32	256	1.0	0.6	1.0	0.50	0.6	0.50	8.0	4.0	12.0	1.0	20,000	1666
C37	32	32	256	1.0	0.6	1.0	0.75	0.6	0.75	8.0	6.0	14.0	1.0	43100	3078.57
C38	32	32	256	1.0	0.6	1.0	1.0	0.6	1.0	8.0	8.0	16.0	1.0	17150	1071.88
C39	32	32	256	1.0	0.6	1.0	1.5	0.6	1.5	8.0	12.0	20.0	1.0	4200	210
C40	32	32	256	1.0	0.6	1.0	2.0	0.6	2.0	8.0	16.0	24.0	1.0	1760	73.33
C41	32	32	256	1.0	0.6	1.0	4.0	0.6	4.0	8.0	32.0	40.0	1.0	940	23.5
C42	32	32	256	1.0	0.6	1.0	8.0	0.6	8.0	8.0	64.0	72.0	1.0	1370	19.02
C43	256	256	256	1.0	0.2	1.0	0.5	0.2	0.5	1.0	0.5	1.5	1.0	3550	2366.6
C44	256	256	256	1.0	0.2	1.0	0.5	0.2	0.5	1.0	0.5	1.5	1.33	4660	3110
C45	256	256	256	1.0	0.2	1.0	0.5	0.2	0.5	1.0	0.5	1.5	1.66	[illegible]	[illegible]
C46	256	256	256	1.0	0.2	1.0	0.5	0.2	0.5	1.0	0.5	1.5	2.00	[illegible]	[illegible]
C47	256	256	256	1.0	0.2	1.0	0.5	0.2	0.5	1.0	0.5	1.5	4.00	[illegible]	[illegible]